Science of Sintering, **53** (2021) 187-198

https://doi.org/10.2298/SOS2102187N

UDK: 678.7; 532.74; 677.017.5; 546.57

Structural and Optical Properties of HDPE Implanted with Medium Fluences Silver Ions

Miloš Nenadović[1*)], Danilo Kisić[1], Miljana Mirković[2], Snežana Nenadović[2], Ljiljana Kljajević[2]

[1]Department of Atomic Physics, Vinča Institute of Nuclear Sciences-National Institute of the Republic of Serbia, University of Belgrade, Serbia

[2]Department of Materials Science, Vinča Institute of Nuclear Sciences- National Institute of the Republic of Serbia, University of Belgrade, Serbia

Abstract:

The implantation of high-density polyethylene (HDPE) has been conducted using Ag^+ ions with energy of 60 keV, achieved fluences 1.5 and $10 \cdot 10^{15}$ ions/cm^2. Transmission electron microscopy (STEM) and field emission gun – scanning electron microscopy (FEG-SEM) showed the existence of nanoparticle clusters. X ray photoelectron spectroscopy (XPS) revealed the presence of silver in the sample surface region. The surface topography was studied by atomic force microscopy (AFM), while the surface composition uniformity was analyzed using phase imaging AFM. Optical characterization obtained by spectroscopic ellipsometry (SE) showed changes in refractive index, extinction coefficient and the optical band gap with the fluence of implanted ions.

Keywords*: Ag ion implantation; Polymers; TEM; Spectroscopic ellipsometry; Optical band gap.*

1. Introduction

For devices possessing optical properties, control of projected range and cluster size of implanted ion species, with refractive indexes of the changed surface is of major importance and determines their optical behavior. Usually, these functional materials properties can be controlled by changing the fluence and implantation energy. In this way, one can control the properties of the resulting dielectric composite metal – polymer, using the combination of different parameters change brings new properties to the final device. Nanosized metal particles posses unique electronic, optical, magnetic, thermal and catalytic properties that are different considerably from that of the bulk phase [1-3]. It comes from small sizes and high surface/volume ratios. Ion implantation of polymers with noble metal ions and formation of nanoparticles is an attractive process to take advantage of these properties. The doped polymer matrices have long term stability [4, 5], which make them suitable for applications in nanoelectronic devices, sensors, molecular optical devices, optoelectronic applications and engineering nanocomposites with well defined properties [6–8]. Silver nanoparticles (Ag NPs) have received considerable attention due to their chemical stability, good thermal, electrical conductivity and catalytic properties. Silver nanoparticles can be synthesized using various methods such as chemical, electrical [9], c-radiation [10], photochemical [11], and laser ablation [12]. Ion implantation is proven to be a highly

*) **Corresponding author:** milosn@vinca.rs

advanced technique for modifying the polymer subsurface region with silver ions. According to the analysis of Atomic Force Mircroscopy (AFM) phase images, surface modification of High Density Polyethilene (HDPE) using silver ions showed significant changes of its surface composition [13]. In the present work, we investigate the effect of Ag ions implantation on optical band gap energy in HDPE/Ag system using spectroscopic ellipsometry (SE). This powerful and nondestructive technique is suitable to investigate the optical response of materials, to measure simultaneously the thickness and dielectric function of a metal – polymer system. The two experimental quantities which are directly obtained through this technique are angles ψ and Δ. These parameters indicate the relative changes of the amplitude and the phase of a linearly polarized monochromatic incident light upon an oblique reflection from a sample surface. These are related to the optical and structural properties of the samples and defined by [14].

$$\rho = \frac{Rp}{Rs} = \tan\psi e^{i\Delta} \qquad (1)$$

where R_p and R_s are the complex reflection coefficients of the light polarized parallel and perpendicular to the plane of incidence, respectively. In this paper, the changes of the refractive index (n) and extinction coefficient (k) with wavelength were investigated. Further analysis of the obtained data provides information on the modification of the optical band gap with the ion fluence.

2. Materials and Experimental Procedures

2.1 Sample preparation

Commercial 2 mm thick sheet of HDPE (0.945 g/cm^3, BASF) was mechanically polished with 4000 grade polishing paper and treated with ethanol in an ultrasonic bath during 20 minutes.
After that, the HDPE plates were washed with ultra pure water which has a resistance of 18.2 MΩ. Finally, sheet was cut into 2 x 2 cm samples and they were placed in the implantation chamber.

2.2 Ion implantation

HDPE samples were implanted using Ag^+ ions with energy of 60 keV in ion implanter chamber. The working pressure in the chamber was constant $1\cdot10^{-5}$ Pa [15, 16]. The source of silver ions was the preheated silver fluoride - AgF salt (Fluka, p.a.). The total amount of implanted ions was: 1, 5 and $10\cdot10^{15}$ ions/cm^2. The working temperature of the sample was kept constant at 20 ^{o}C using the target cooling system.

2.3 Characterization of samples

2.3.1 Electron microscopy

Transmission electron microscopy (TEM) was performed on a TEM microscope Jeol ARM 200 CF at an accelerating voltage of 200 keV. Medium thick cross-sections (about 10 μm) were cut from HDPE bulk top side and transferred to the TEM grids. Those grids were placed in liquid nitrogen cryo stage (77 K) so the samples become conductive when interacting with the electron beam. Scanning electron microscopy (SEM) was carried out on FEI Helios Nanolab 650 equipped with Focused Ion Beam/Field Emission Gun as additional equipment. Focused ion beam sputtered the sample surface until it reached the projected range of the implanted silver ions. The instrument has superb imaging capabilities, providing sub-

nanometer resolution across the whole 1-30 kV range. It's through-the-lens detector sets collection efficiency of both secondary electrons (SE) and on-axis backscattered electrons (BSE), and is complemented by two multi-segment solid state detectors, a detector for backscattered electron (BSE). The system is equipped with a state-of-the-art XEDS Silicon Drift Detector (SDD) system by Oxford Instruments, with energy resolution of 125 eV for Mn Kα (5.899 keV) using for elemental analysis of the sample.

2.3.2 AFM imaging

Multimode quadrex SPM with Nanoscope IIIe controller (Veeco Instruments, Inc.), operated under ambient conditions was used in this investigation. Surface topography and phase images were simultaneously acquired by standard AFM tapping mode using a commercial NanoScience-Team Nanotec GmbH SNC (Solid Nitride Cone) AFM probe, with the tip radius smaller than 10 nm.

2.3.3 X-ray photoelectron spectroscopy (XPS)

The surface chemical analysis was acquired using a SPECS system for X-ray photoelectron spectroscopy, consisting of a hemispherical analyzer PHOIBOS 100 ver.4.0 and X-ray source XR 50 M equipped with a monochromator SPECS FOCUS 500. Photoelectron emission has been excited by monochromatic Al K_α line having photon energy equal to 1486.67 eV. Survey spectra were taken in a fixed analyzer transmission mode with pass energy of 40 eV (FAT 40), energy step of 0.5 eV and the dwell time of 0.2 s. Detailed spectra of the main photoelectron lines were taken in FAT 20 mode with the energy step of 0.1 eV and the dwell time of 2 s.

2.3.4 Spectroscopic Ellipsometry (SE)

The ellipsometric measurements were done using HORIBA Jobin Ivon, monochromatic device iHR- 320 at room temperature, under incident angle of 70° in the wavelength range from 200 to 2200 nm (photon energy range from 0.6 to 4.8 eV). Fitting the model to the experimental curve was estimated using the double Tauc–Lorentz (DTL) model, with the analytical parameters which are simultaneously determined through the iterative process change until the error function obtains the minimum value:

$$\chi^2 = min \sum_{i=1}^{n} \left[\frac{(\Psi_{theor} - \Psi_{exp})_i^2}{\Gamma_{\Psi,i}} + \frac{(\Delta_{theor} - \Delta_{exp})_i^2}{\Gamma_{\Delta,i}} \right] \qquad (2)$$

In the above expression, n is the total number of recorded points (Ψ_{exp}, Δ_{exp}), while (Ψ_{theor}, Δ_{theor}) are experimental values of ellipsometrical angles and corresponding values calculated from the model using a parameter $\Gamma_{\Delta,i}$ for calculation of the experimental error. All calculations were performed using DeltaPsi 2 software package, which is an integral part of the device.

3. Results and Discussion

3.1 Electron microscopy analysis

Transmission electron microscopy was carried out on samples HDPE/Ag implanted with fluence $1 \cdot 10^{16}$ ions/cm^2. It is performed by the method HAADF/STEM: high-angle annular dark field/scanning transmission electron microscopy that revealed the existence of spherical nanoparticles with diameter in the range from 5 to 10 nm (Fig. 1a and b). Silver

nanoparticles are grouped in clusters and there is no coalescence of particles. The reason for this is that the implantation fluence is in the range of medium fluence, where clusters remain separated.

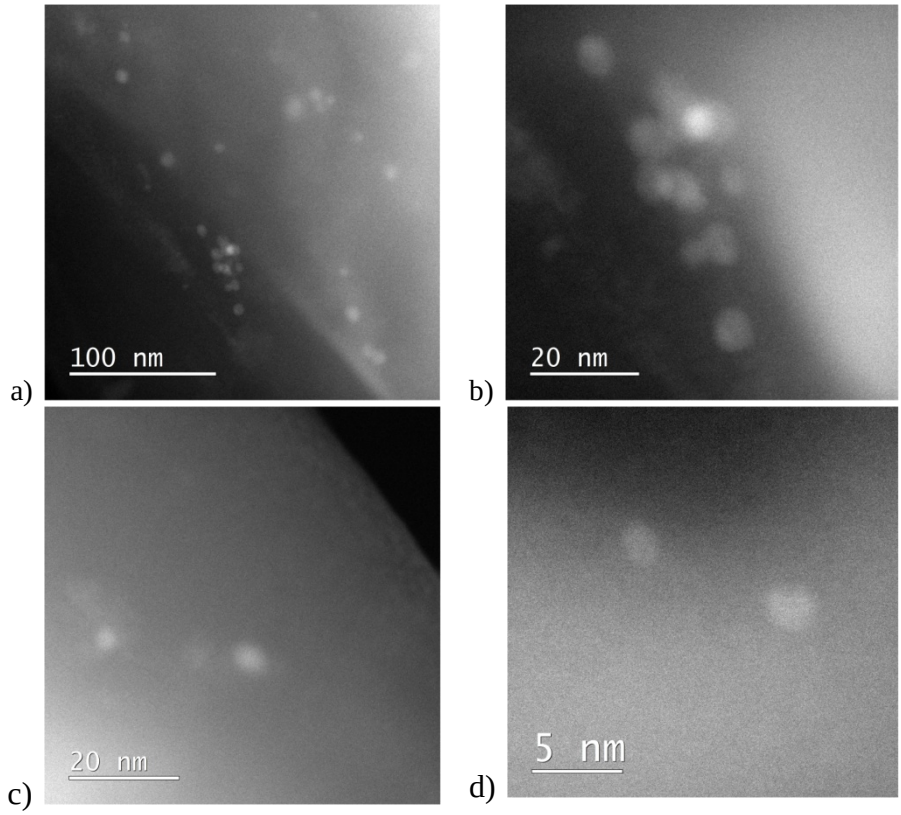

Fig. 1. STEM/HAADF image of silver nanoparticles in high density polyethylene.

However, important for this study were just medium implantation fluences ($1 \cdot 10^{15}$ ions/cm^2, $5 \cdot 10^{15}$ ions/cm^2 and $1 \cdot 10^{16}$ ions/cm^2), leading to substantial optical changes in the polymer.

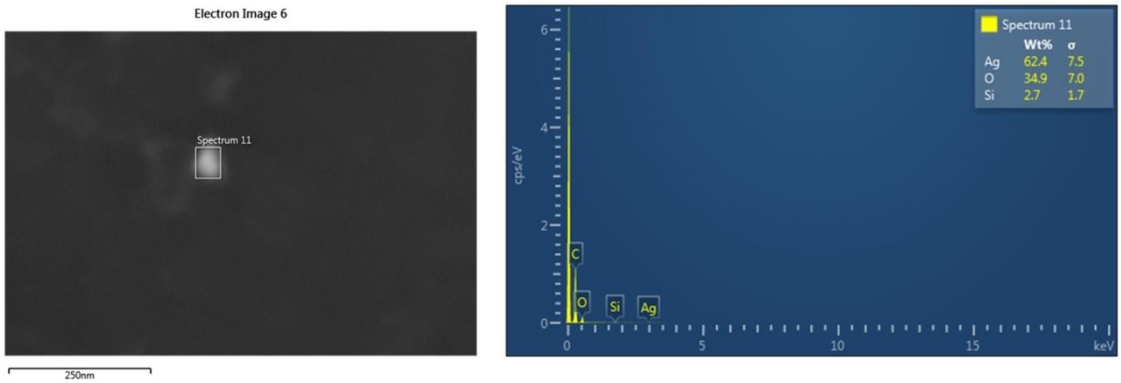

Fig. 2. a) FIB/FEG SEM analysis of silver nanoparticles in HDPE; b) EDXS elemental analysis of HDPE/Ag sample.

Scanning electron microscopy also confirmed the presence of silver nanoparticles embedded in a polymer structure (Fig. 2a). Using the system FIB/FEG SEM-Focused Ion Beam/Field

Emission Gun SEM microscope sputtered surface layers of HDPE given another confirmation of incorporation of silver nanoparticles into a polymer matrix. Elemental analysis was done using EDXS analysis (Fig. 2b).

Under the assumption of in-depth uniform sample the atomic percentages of impurities, i.e. non-carbon species, is Ag:O:Si = 20.2:76.4:3.3. Since silver is implanted at several tens of nanometers below the surface, its signal is highly attenuated with respect to that of oxygen which is a surface impurity (see below). Consequently, the actual amount of silver is underestimated.

3.2 XPS analysis of HDPE and HDPE/Ag samples

Sputtering by 1 keV Ar^+ ions for about 30 seconds reduced significantly oxygen signal in the XPS spectra, clearly revealing that it general represents a surface contamination. Apart from the etching of the surface oxidized layer, another consequence of Ar sputtering is its implantation. The evidence of the later can be observed from the presence of Ar 2p line in the survey spectra taken after the ions sputtering (Fig. 3). Other photoelectron lines readily observed are those of carbon and oxygen in the pristine HDPE (Fig. 3a), but also of silver in the implanted sample (Fig. 3b). The relative amount of oxygen at the surface is about 1.6 % in both samples, whilst that of silver in the implanted sample is only 0.1 %. Very low concentration of silver should not be a surprise having in mind the position and FWHM of the implantation profile. Having in mind high surface sensitivity of XPS, much larger ratio of O and Ag concentrations by this technique than in the case of EDSX analysis is another indication that oxygen is situated dominantly at the samples' surface.

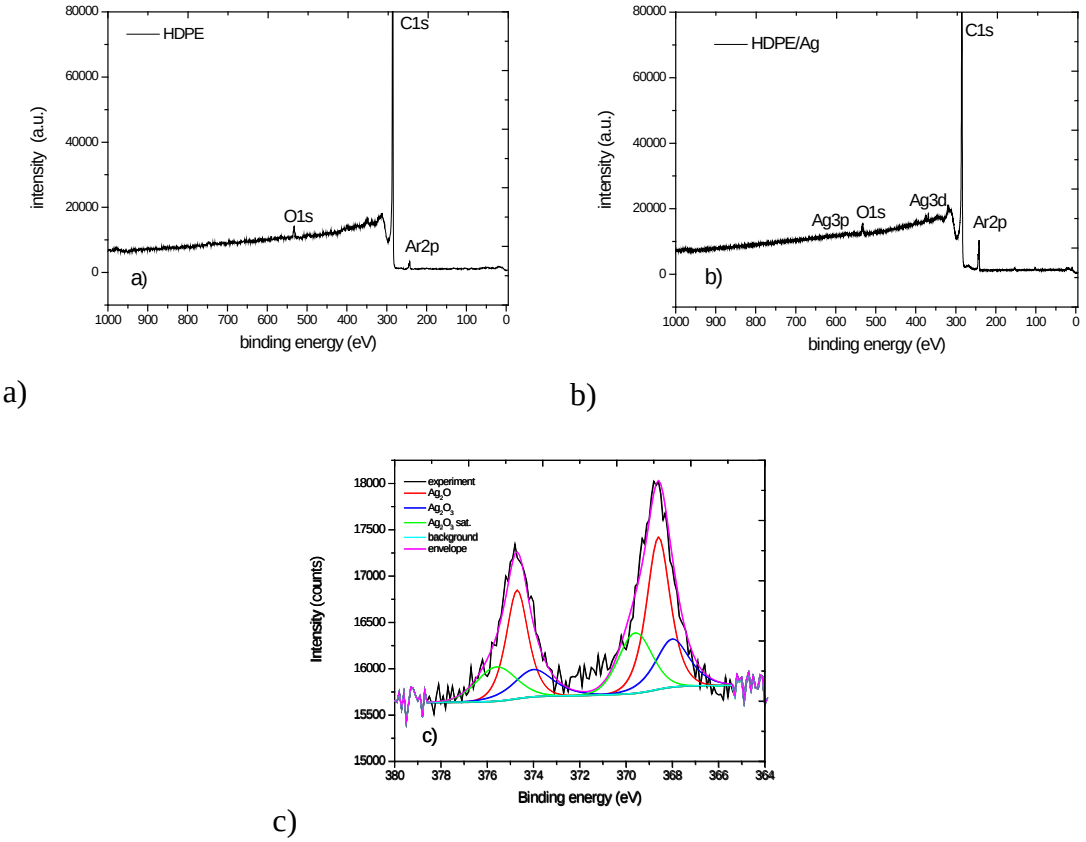

Fig. 3. X-ray photoelectron spectroscopy spectra: a) HDPE; b) HDPE/Ag implanted with fluence $1 \cdot 10^{16}$ ions/cm^2; c) Ag 3d detailed spectra.

The binding energy axis, which was shifted due to the sample charging, was calibrated by putting the C 1s line at 285.0 eV, assuming it corresponds to HDPE. Under this assumption, O 1s line in both samples is situated at 532.9 eV, which fits very well with the C-OH bonds [17].

The position of the main silver photoelectron line Ag $3d_{5/2}$ at about 368.8 eV and its relatively large width suggest that silver at the surface is not in the metallic state. Very good fit of the Ag 3d line was obtained for the AgO phase, presented in Fig. 3c. As it is known from the magnetic measurements, this compound actually represents the mixture of Ag_2O and Ag_2O_3. The first dominant narrow peak in the Ag $3d_{5/2}$ line at 368.6 eV corresponds to the first phase. The other two contributions at 368.0 and 369.6 eV represent the main peak of the Ag_2O_3 phase, and its shake-up satellite. The constraints between the three contributions concerning their relative intensities and positions, as well the peak widths are based on the XPS measurements of a reference AgO sample [18]. The formation of the AgO phase at the sample surface is most probably related to the increased oxygen content in this region. However, this result does not provide any information on the phase of silver nanoparticles in the bulk.

3.3 AFM surface analysis of HDPE and HDPE/Ag samples

Characteristic topographic and phase analysis of the HDPE and HDPE/Ag surfaces was performed using AFM microscope. The virgin HDPE (Fig. 4a) shows the existence of large grains on the surface, which become even more evident in the AFM phase image (Fig. 4b). Grains are pretty large (about half a micrometer and more) and the grain boundaries are clearly observed.

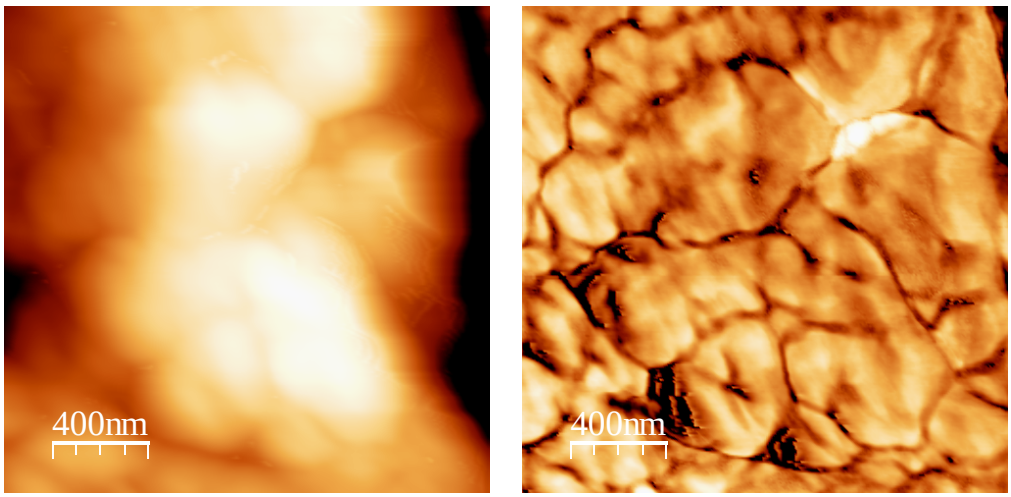

a) b)

Fig. 4. a) AFM topographic analysis of unimplanted HDPE, b) AFM phase analysis of unimplanted HDPE (2 x 2 μm); Z – range 10 nm.

Ag^+ ion implantation using the fluence of $1 \cdot 10^{16}$ ions/cm^2 resulted in significant change of the HDPE surface. (Fig. 5). Topographic AFM image (Fig. 5a) shows the presence of radiation-damage pronounced peaks, while the phase image (Fig. 5b) more clearly reveals small grains ordered in chains.

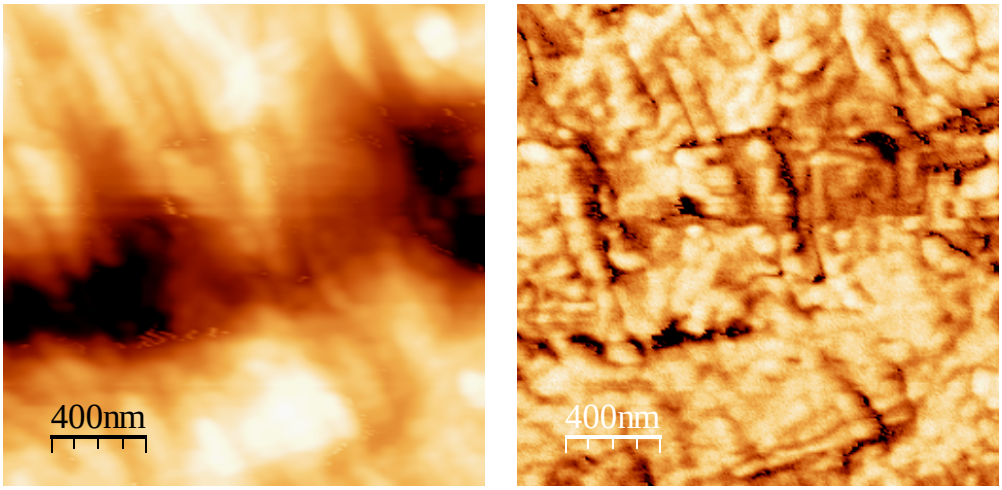

a) b)

Fig. 5. a) AFM topographic analysis of HDPE/Ag $1\cdot10^{16}$ ions/cm^2, b) AFM phase analysis of HDPE/Ag $1\cdot10^{16}$ ions/cm^2 (2 x 2 μm); Z – range 40 nm.

Atomic force microscopy – force modulation microscopy (AFM-FMM) [19] cross section image (Fig. 6a) is compared with Stopping and Range of Ions in Matter (SRIM-2006) (Fig. 6b). SRIM calculation predicted projected range of 60 keV silver ions at about 65 nm of depth, with FWHM of 30 nm.

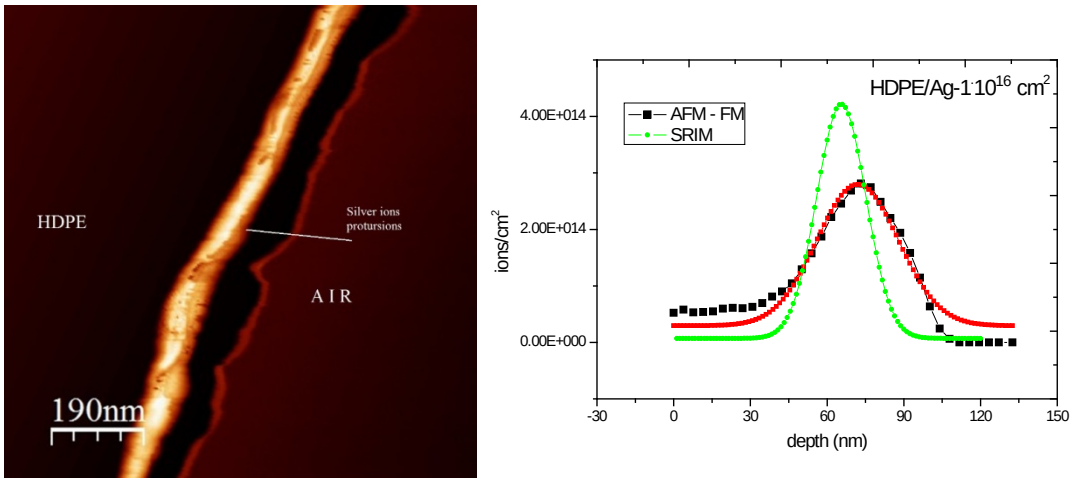

a) b)

Fig. 6. a) AFM-FMM image of cross-section HDPE/Ag; b) Comparison of experimental (AFM-FMM) cross section and calculated (SRIM) profile of HDPE/Ag.

Experimentally obtained results using AFM-FMM method showed slightly deeper penetration of silver ions, with the projected range at about 75 nm and FWHM of 45 nm. The damage produced by silver ions make moving projected range toward depth also widening the FWHM of implanted silver. This behavior can be attributed to a radiolysis of polymer and radiation enhanced diffusion [20-24].

3.4 Ellipsometric spectroscopy analysis

Degree of optical changes on the high-density polyethylene surface due to silver ion implantation using fluences from $1\cdot10^{15}$, $5\cdot10^{15}$ up to $1\cdot10^{16}$ ions/cm^2 are shown in Fig. 7 (a, b). Fig. 7a shows the dependence of the refractive index (*n*) on the wavelength. For unimplanted HDPE sample one can see almost constant value of refractive index depending on the wavelength and has a value of about 1.5. This indicates the existence of homogeneity in the HDPE structure because there is no significant change the speed of light through polymer and therefore the refractive index change. Silver ion implantation in high density polyethylene leads to significant changes in the optical spectra and properties. Implantation fluence of $1\cdot10^{15}$ ions/cm^2, shows a refractive index maximum at a wavelength of 420 nm and amounts 1.94. That maximum increases with increasing the implantation fluence at $5\cdot10^{15}$ ions/cm^2 and amounts 2.15 at a wavelength of 482 nm. The same trend applies for the highest implantation fluence of $1\cdot10^{16}$ ions/cm^2, where the refraction index maximum occurs at a wavelength of 596 nm and amounts 2.32.

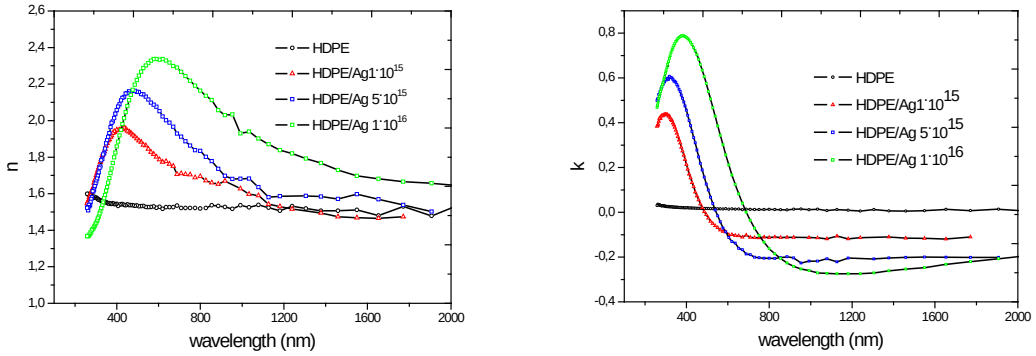

a) b)

Fig. 7. The optical spectra of the system HDPE/Ag implanted with fluence $1\cdot10^{15}$, $5\cdot10^{15}$ and $1\cdot10^{16}$ ions/cm^2: a) the dependence of *n* on the wavelength b) the dependence of *k* on the wavelength.

The obvious trend is the increase and shifting of the refractive index maximum towards longer wavelengths with increasing implantation fluences. A higher concentration of silver ions in the polymer represents a major obstacle to the propagation of light through the material and therefore the refraction index value increases with the implantation fluence. Fig. 7b presents the dependence of the extinction coefficient (k) on the wavelength. For virgin sample, one can see a constant value of the extinction coefficient, close to zero, irrespective to the value of the wavelength. This indicates a high degree of HDPE transparency, in the entire wavelength range. Implanting different fluences of silver ions leads to the appearance of a similar trend as for the refraction index. In the case of the lowest ion fluence of $1\cdot10^{15}$ ions/cm^2, the extinction coefficient reaches maximum of 0.41 at 304 nm. In the case of the ion fluence of $5\cdot10^{15}$ ions/cm^2, the extinction coefficient maximum is shifted to 323 nm and amounts 0.59. For the highest silver ion fluence of $1\cdot10^{16}$ ions/cm^2, the extinction coefficient has a value of 0.79 at a wavelength of 389 nm. Extinction coefficient is a measure of the material optical absorption. In the case of different fluences silver ions implantation, there is an increase of absorption rate with increasing the implantation fluence. This is in accordance with expected results because the amount of material implanted is directly proportional to the degree of absorption. This absorption band can be attributed to the surface plasmon resonance (SPR) absorption of Ag nanoparticles [25]. The appearance of the SPR band indicates that Ag

nanoparticles were formed in the samples after the implantation. The formation of Ag particles is previously confirmed by STEM/HAADF investigation (shown on Fig. 1). As shown in Fig. 7 (a,b) the position of the SPR band in the samples is shifted towards longer wavelength when increasing the Ag ion fluence. The intensity of the SPR absorption band in samples also increases with fluence, which can be a consequence of the increase of silver concentration and/or the size of Ag nanoparticles. Average radius of Ag nanoparticles can be calculated using the equation [26]:

$$R = \frac{Vf}{\Delta\omega 1/2} \qquad (3)$$

where V_f is the Fermi velocity of the electrons in the metal, $\Delta\omega_{1/2} = 2\pi c\,(\Delta\lambda/\lambda p^{2})$ and $\Delta\lambda$ is the full width at half maximum wavelength and λ_p the peak wavelength, obtained from the optical spectra. Taking for $V_f = 1.45\cdot10^{6}$ m/s and the calculated $\Delta\omega_{1/2}$ this formula gives the average radius of Ag particles: 2 ± 0.7 nm for HDPE/Ag - $1\cdot10^{15}$ ions/cm^2 ; 4 ± 1.5 nm for HDPE/Ag - $5\cdot10^{15}$ ions/cm^2 and 8 ± 3 nm for HDPE/Ag - $1\cdot10^{16}$ ions/cm^2 (shown on Fig. 1).

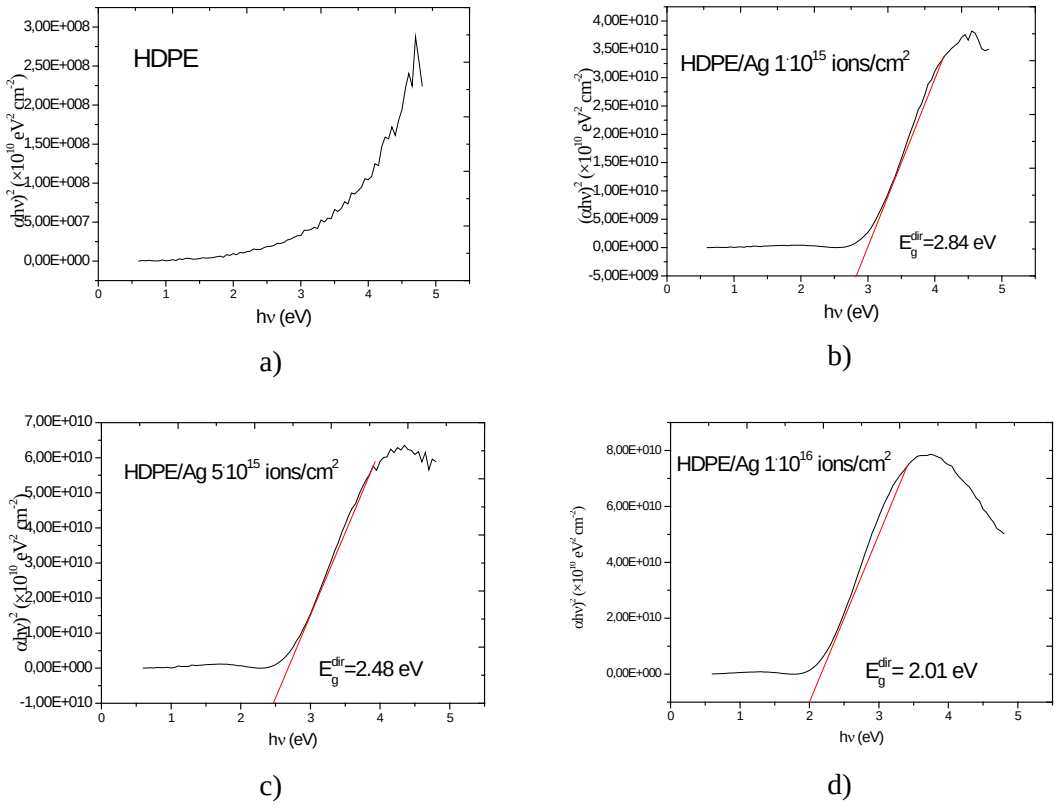

Fig. 8. Dependence of $(ahv)^2$ vs hv for determination of direct optical band gap energy (E_g^{dir}) a) virgin HDPE (no gap), b) HDPE/Ag - $1\cdot10^{15}$ ions/cm^2 , c) HDPE/Ag - $5\cdot10^{15}$ ions/cm^2 , d) HDPE/Ag - $1\cdot10^{16}$ ions/cm^2.

The direct optical band gap energy (E_g^{dir}) of the HDPE and HDPE/Ag implanted samples was extracted from the spectral dependence of the absorption coefficient a by applying the following relations:

$$(ahv)^2 = const.\,(hv - E_g^{dir}) \qquad (4)$$

and

$$\alpha = \frac{4\pi k}{\lambda} \qquad (4a)$$

where *hv* is the energy of the incident radiation. The plots between $(ahv)^2$ vs *hv* (known as Tauc plots) for different silver ions fluences are presented in Fig. 8. The value of the direct optical energy gap E_g^{dir} was estimated from the plot between $(ahv)^2$ vs *hv* (Fig. 8.) by extrapolating the linear portion of the Tauc plot to $(ahv)^2 = 0$.

The value of E_g^{dir} (direct transitions) decreased (Fig. 8.) with increase of the silver ion fluence. The decrease of the band gap may be due to the increase oh the structural disorder or defects generated due to the ion implantation that formed silver nano-clusters confirmed earlier using (SEM, TEM). Furthermore, the defects are created because of several factors, but the most important are radiation damage and very high local heating through latent tracks [26-30]. As a final result, the optical gap decreases slightly due to the increase of disorder and silver cluster defects in the polymer matrix. Probably, isolated electrically charged nano-clusters, when present in the polymer structure, give rise to an electric field within the bulk polymer. The internal fields thus produced strongly affect the band structure [27-33]. The increase of disorder and radiation damage defects in the structural polymer bonding with increasing silver ion fluences in HDPE results in decrease of optical band gap.

4. Conclusion

Silver ion implantation in high density polyethylene (HDPE) has been used as most convenient to modify near surface structural and optical properties. The chosen ion fluences were in the range of medium 1.5 and $10 \cdot 10^{15}$ ions/cm^2 in order to obtain silver nano-clusters from 5 to 10 nm. Transmission electron microscopy (STEM) and field emission gun – scanning electron microscopy (FEG-SEM) confirmed the existence of silver nanoparticles and small clusters affecting on the optical response of the system HDPE/Ag. X ray photoelectron spectroscopy (XPS) revealed the presence of implanted silver in the near surface region. The surface topography was observed by atomic force microscopy (AFM), while the surface composition changes were analyzed using phase imaging AFM. Optical characterization obtained using spectroscopic ellipsometry (SE) verified the significant changes in refractive index, extinction coefficient and revealed decrease in the optical band gap with increasing the implantation fluence.

Acknowledgments

This work was financially supported by the Ministry of Education and Science of the Republic of Serbia.

5. References

1. J. M. Charrier, Polymeric Materials and Processing: Plastics, Elastomers and Composites, Hanser Publishers, Munich, New York, 1991.
2. A. Kondyurin, M. Bilek, Ion Beam Treatment of Polymers: Application Aspects from Medicine to Space, Elsevier, Oxford, UK, 2008.
3. L. M. Liz-Marzan, Mater. Today 26 (2004) 31
4. D. Y. Godovsky, Adv. Polym. Sci. 119 (1995) 79.

5. L. L. Beecroft, C. K. Ober, Chem. Mater. 9 (1997) 1302.
6. Z. Tang, N. A. Kotov, S. Magonov, B. Ozturk, Nat. Mater. 2 (2003) 413.
7. J. J. Schneider, Adv. Mater. 13 (2001) 529.
8. L. Calcagno, G. Compagnini, G. Foti, Nucl. Instrum. Methods B 65 (1992) 413.
9. S. A. Vorobyova, A. I. Lesnikovich, N. S. Sobal, Colloid Surface A 152 (1999) 375.
10. S. H. Choi, Y. P. Zhang, A. Gopalan, K. P. Lee, H. D. Kang, Colloid Surface A 256 (2005) 165.
11. Z. Li, Y. Li, X. F. Qian, J. Yin, Z. K. Zhu, Appl. Surf. Sci. 250 (2005) 165.
12. T. Tsuji, N. Watanabe, M. Tsuji, Appl. Surf. Sci. 211 (2003) 189.
13. S. Strbac, M. Nenadovic, Lj. Rajakovic, Z. Rakocevic Appl. Surf. Sci. 256 (2010) 3895
14. H. Fujiwara, Spectroscopic Ellipsometry: Principles and Applications, John Wiley & Sons Ltd., 2007.
15. M. Nenadović, J. Potočnik, M. Ristić, S. Štrbac, Z. Rakočević, Surface modification of polyethylene by Ag^+ and Au^+ ion implantation observed by phase imaging atomic force microscopy, Surface and Coatings Technology, 206 (2012) 4242-4248.
16. M. Nenadović, J. Potočnik, M. Mitrić, S. Štrbac and Z. Rakočević, Modification of high density polyethylene by gold implantation using different ion energies, Material Chemistry and Physics, 142 (2013) 633-639.
17. G. Beamson, D. Briggs, High Resolution XPS of Organic Polymers – The Scienta ESCA300 Database, Wiley Interscience, New York, 1992.
18. A. M. Ferraria, A. P. Carapeto, A. M. B. do Rego, X-ray photoelectron spectroscopy: silver salts revisited, Vacuum 86 (2012) p. 1988-1991
19. S. Strbac, M. Nenadovic, Lj. Rajakovic, Z. Rakocevic, Appl. Surf. Sci. 256 (2010) 3895-3899
20. D. Kisic, M. Nenadovic, T. Barudžija, P. Noga, D. Vana, M. Muška, Z. Rakocevic, Modification of polyethylene surface properties by high fluence Fe implatantion, Nucl. Instrum meth B, (2020) 143-153
21. D. Kisic, M. Nenadovic, J. Potocnik, M. Novakovic, P. Noga, D. Vana, A. Zavacka, Z. Rakocevic, Surface layer morphology of the high fluence Fe implanted polyethylene-correlation with the magnetic and optical behavior, Vacuum 171 (2020) 109016
22. A. Modric-Sahbazovic, M. Novakovic, E. Schmidt, N. Bibic, I. Gazdic, C. Ronning, Z. Rakocevic, Thermal Annealing of Ag Implanted Silicon: Relationship between Structural and Optical Properties, Sci Sinter, 52 (2020) 207-217.
23. J. Potocnik, M. Nenadovic, B. Jokic, M. Popovic, Z. Rakocevic, Structural, Chemical and Magnetic Properties of Nickel Vertical Posts Obtained by Glancing Angle Deposition Technique, Sci. Sinter, 49(2017) 73-79.
24. L. H. Zhou, C. H. Zhang, Y. T. Yang, B. S. Li, L.Q. Zhang, Y. C. Fu, H. H. Zhang, Nucl. Instrum. Methods B 267 (2009) 58-62.
25. M. K. Patel, B. J. Nagre, D. M. Bagul, Surf. Coat. Technol. 196 (2005) 96.
26. V. N. Popok, Rev. Adv. Mater. Sci. 30 (2012) 1.
27. Prikshit Gautam, Anupama Sachdeva, Sushil K. Singh, R. P.Tandon, Jour. of All. and Comp. 617 (2014) 374-378.
28. G. Pan, R. Kesavamoorthy, S. A. Asher, Nanosecond switchable polymerized crystalline colloidal array bragg diffracting materials, J. Am. Chem. Soc. 120 (1998) 6525-6530.
29. J. M. Weissman, H. B. Sunkara, A. S. Tse, S. A. Asher, Thermally switchable periodicities and diffraction from mesoscopically ordered materials, Science 274 (1996) 959-960.

30. H. Holland-Moritz, A. Ilinov, F. Djurabekova, K. Nordlund, C. Ronning, Sputtering and redeposition of ion irradiated Au nanoparticle arrays: direct comprasion of simulations to experiments, New J. Phys. 19 (2017) 013023.
31. H. M. Urbassek, M. L. Nietiadi, R. M. Bradley, G. Hobler, Sputtering of SicGe1−c nanospheres, Phys. Rev. B 97 (2018) 155408.
32. J. Wang, G. Wang, C. L. Liu, Plasmonic behaviors of two-dimensional Ag/SiO_2 nanocomposite gratings: roles of gap diffraction and localized surface Plasmon resonance absorption, Plasmonics 14 (2019) 921-928.
33. H. X. Liu, X. D. Zhang, Y. Y. Shen, L. H. Zhang, J. Wang, F. Zhu, B. Zhang, C. L. Liu, Tailoring the size distribution of Ag nanoparticles embedded in SiO_2 by Xe ion postirradiation, APEX 5 (2012) 105002.

Сажетак: *Јони Ag^+ су имплантирани у полиетилен велике густине (ПЕВГ) енергијом од 60 keV, дозама 1.5 и $10{\cdot}10^{15}$ јона/cm^2. Трансмисиона електронска микроскопија (STEM) и скенирајућа електронска микроскопија (FEG-SEM) показале су постојање кластера наночестица. Рендгенском фотоелектронском спектроскопијом (XPS) откривено је присуство сребра на површини узорка. Топографија површине проучавана је микроскопијом атомских сила (AFM), док је униформност састава површине анализирана помоћу АФМ за фазно снимање. Оптичка карактеризација спектроскопском елипсометријом (SE) показала је промене индекса преламања, коефицијента екстинкције и опсега оптичког појаса са дозама имплантираних јона.*
Кључне речи*: Ag јонска имплантација, полимери, TEM, спектроскопска елипсометрија, оптички појас.*